Sensors and Materials, Vol. 12, No. 1 (2000) 035–055
MYU Tokyo

S & M 0395

A Humidity Sensor Featuring a Porous Silicon Capacitor with an Integrated Refresh Resistor

Zacharias M. Rittersma and Wolfgang Benecke

University of Bremen, Faculty of Physics and Electrical Engineering
Institute for Microsensors, Actuators and Systems (IMSAS)
PO Box 330 440, D-28334 Bremen, Germany

(Received December 24, 1999; accepted March 15, 2000)

Key words: humidity sensor, porous silicon, refresh resistor

A capacitive humidity sensor featuring a porous silicon dielectric film is described. The device consists of a parallel-plate capacitor with a meshed top electrode, two metal resistors for measuring the temperature of the sensor, and a metal refresh resistor. With the integrated resistors, the humidity measurement can be corrected for cross sensitivity of temperature. With the refresh resistor, the sensor can be heated and hence the amount of vapour adsorbed can be controlled. In normal operation, this tool can be used to improve the long-term stability of the device, as well as to minimise hysteresis effects. The general design considerations which led to the design are presented, as well as effective medium approximations that describe the as-measured permittivity of a porous silicon dielectric which is partly filled with condensed vapour. In addition to the fabrication of the sensor, measurements are presented which demonstrate the humidity-sensitive properties of the porous silicon capacitor, the temperature compensation and the influence of the electrical power supplied to the refresh resistor on the humidity-sensitive properties of the porous silicon.

1. Introduction

The material porous silicon is gaining increasing attention in microsystem technology (MST). The research on porous silicon in the late 1980s and early 1990s focused on the relation between formation parameters and morphology,[1–3] as well as on different techniques to form porous silicon. It is now well known that porous silicon is best formed by electrochemical etching of single crystal silicon in concentrated hydrofluoric acid (HF)

under low anodic bias. Though some aspects of this formation process still remain to be clarified, the relation between the parameters of the electrochemistry —current density, dopant level of the silicon, HF concentration— and the pore structure or morphology that is obtained is widely known.[4] The morphology is characterised by the void fraction or porosity, ξ, the mean size of the pores, the pore size distribution, the interconnectivity of the pores, and finally by the passivation and mean size of the skeleton enclosing the pores. Porous silicon formed in low-doped (2–10 Ωcm) silicon exhibits a sponge-like structure with highly interconnected pores and wires in the nm range, whereas that formed in high-doped (< 2 Ωcm) silicon exhibits on average larger, preferentially oriented pores with numerous smaller side branches.[4] The history of porous silicon research is quite remarkable. This material has been disregarded for several years after it was accidentally discovered by Ulhir in 1956,[5] but currently a wide variety of applications in MST are being investigated. Examples of these applications are the use of porous silicon as a (thick) sacrificial layer[6,7] and as a coupling matrix in biochemical microsystems.[8] Porous silicon has also been investigated for its luminescence properties, which make it possibly appropriate for many optical applications.[9] At the same time, little or no attention has been paid to the yield or the uniformity of the porous silicon formation process, as applied to the standard processing of single crystal silicon wafers. Furthermore, improvement of the long-term stability of porous silicon by oxidation or impregnation with, for example, noble metals remains a subject for further research.[10,11] In this paper, the design, fabrication and characterisation of a capacitive porous silicon-based humidity sensor is presented. The development of this device was directed by general demands for humidity sensors, but also by economic factors such as yield and reproducibility. Special emphasis was placed on the development of a porous silicon back-end process for optimal control of the properties of the humidity-sensitive capacitor. In a previous work, it was shown that the water uptake of porous silicon can lead to very sensitive humidity-sensitive structures.[12] One of the most interesting problems in applying porous silicon in this application is to find the morphology, i.e., the formation parameters, for the most advantageous sheets.[13] For this reason, effective medium approximations are proposed to understand the water uptake as function of the three-dimensional morphology. Finally, the on-chip integration of resistors and their application is discussed. First, some definitions with respect to humidity measurement are summarised.

2. Humidity Measurement

2.1 *Definitions*

The term 'humidity' refers to the amount of water vapour in a gaseous environment. This can be expressed in several ways, for example, as absolute humidity (χ), as mixing ratio (MR) or as relative humidity (RH). The absolute humidity equals the total water vapour mass present in a volume V:

$$\chi = \frac{N \cdot M_w}{V}, \quad [\mathrm{g/m^3}] \tag{1}$$

where N is the amount of vapour molecules and M_w the molecular mass of H_2O. With p_{tot} the total pressure of the moist system, the mixing ratio in ppm by volume is:

$$MR = \frac{p_w}{p_{tot} - p_w}, \quad [\text{ppmv}] \tag{2}$$

where p_w is the water vapour pressure. The environment can contain only a certain amount of water vapour, above which it is said to be saturated. Experimentally, it has been found that the saturation pressure p_s is an exponential function of the temperature. After conversion of the logarithms as given in mbar, this dependence can be written as:

$$\log p_s = -2937.4 / T - 4.9283 \cdot \log T + 23.5470, \tag{3}$$

where the constants were determined over liquid water and T is the temperature [K]. Determined over ice, these constants are different because the binding forces in ice are stronger than those in liquid water. The RH is defined as the vapour pressure relative to the saturation pressure at a specific temperature:

$$RH = 100 \cdot \frac{p_w}{p_s}. \quad [\%] \tag{4}$$

Another important parameter in humidity measurement is the saturation deficit SD, which is defined as the difference between p_s and p_w:

$$SD = p_s - p_w. \quad [\text{N/m}^2] \tag{5}$$

The SD expresses to what value the vapour pressure of a given amount of gas can be increased —at constant temperature— before condensation will occur. If on the other hand the temperature of a closed volume is decreased, the RH will increase until a point where $p_w = p_s$; the temperature of the gas at this point is called the dew point temperature T_d, or simply the dew point. Formally, T_d is thus implicitly defined by

$$p_s(T_d) = p_w(T). \tag{6}$$

These parameters for humidity measurement are schematically shown in Fig. 1.

2.2 *Dielectric properties of adsorbed water*

A capacitive humidity sensor relies on the change of the electrical properties of a thin film upon adsorption of water vapour. The properties of the sensor are hence determined by those of the adsorbed vapour, by the properties of the thin film and by the design of the electrodes of the capacitor. The polar structure of the H_2O molecule (see Fig. 2) accounts

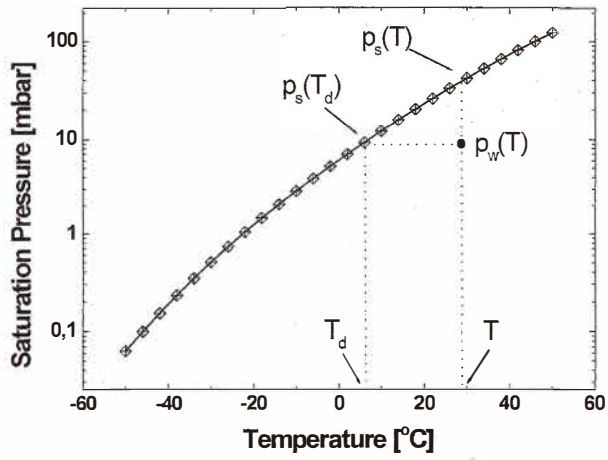

Fig. 1. Saturation pressure of water as function of temperature.

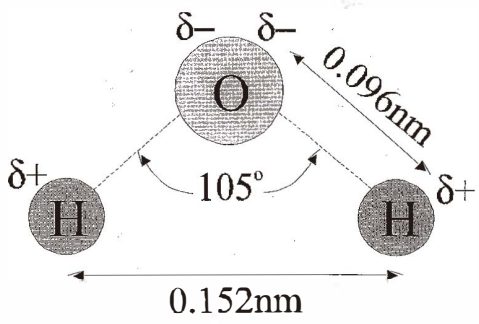

Fig. 2. Schematic of H_2O molecule.

for a high permittivity, $\varepsilon_w \approx 80$, at room temperature. Further, dielectric relaxation of water is expected only above 1.3 GHz.[14] There is, however, a certain temperature dependency of ε_w. Liquid water consists of clusters of H_2O molecules, and the cluster size and consequently also ε_w are a function of T.

$$\varepsilon_w(T) = 87.74 - 0.4 \cdot T + 9.398 \cdot 10^{-4} \cdot T^2 - 1.41 \cdot 10^{-6} \cdot T^3 \quad [-] \tag{7}$$

This effect is neglected here, because it will be very small compared to any possible temperature dependence of the moisture uptake of porous silicon. Furthermore, the properties of adsorbed vapour are in general somewhat different, because of its reduced mobility and because it does not exist in clusters as assumed in eq. (7).

3. Design

3.1 *General considerations*

A comparison of different techniques for humidity measurement given elsewhere[15] led to the following conclusions for the design of a porous silicon humidity sensor: (1) it must be either a capacitance- or a resistance-type sensor, (2) it must be easy to fabricate and to package, (3) it should be as small as possible without making the packaging too critical, (4) the choice of the materials must be such that the sensor can be continuously operated at elevated temperatures, i.e., at least $T = 50°C$ and possibly higher, (5) it should include an integrated refresh unit to improve the long-term stability of the porous dielectric and (6) it should include temperature sensors to compensate for temperature effects on the humidity measurement, as well as to control the refresh.

3.2 *Layout*

A schematic of the humidity sensor is shown in Fig. 3. It consists of a humidity-sensitive parallel plate capacitor formed between a top electrode and the back surface of the sensor (1), a refresh resistor patterned around the capacitor (2) and two high-ohmic resistors for measurement of the sensor's temperature (3). The latter can be used to compensate cross-sensitivity of temperature, for example, the temperature-dependent moisture uptake of the porous silicon (see below). The working principle of this sensor is straightforward: water molecules diffuse from the environment into the porous silicon. Due to the differences in permittivity, the capacitance changes as a function of the moisture uptake, which is directly related to the humidity in the environment. Though

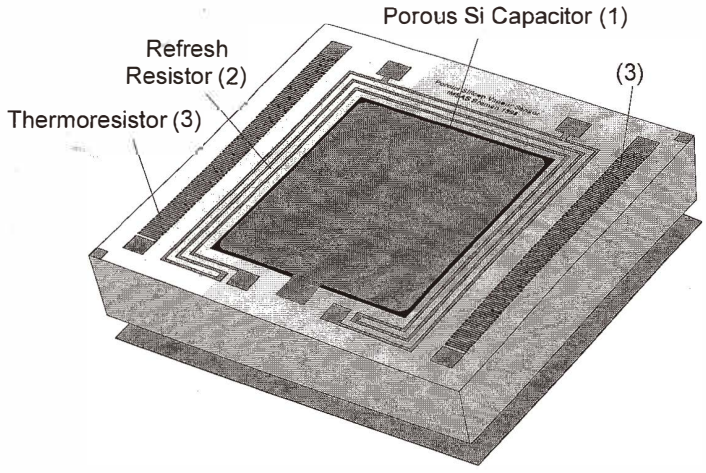

Fig. 3. Schematic diagram of the porous silicon humidity sensor. (1) Capacitor formed between meshed top electrode and back surface of the chip, (2) refresh resistor and (3) metal thermoresistors.

porous materials are advantageous for obtaining high sensitivities, it is well known that the accuracy of humidity measurement with porous materials is limited by *hysteresis* and *drift*. Therefore, a refresh resistor is integrated in this device. With this resistor, it is possible to periodically heat the sensor such that all adsorbed vapour is effectively effused and the porous dielectric is cleaned or 'refreshed'. Furthermore, while keeping the sensor at a constant temperature slightly above the environmental temperature, the amount of vapour adsorbed and the diffusion into the porous silicon can be controlled. This may be used for selectivity enhancement with respect to other vapours.[15] Refreshing can take considerable electrical power, and hence for rapid refreshing it would be advantageous to fabricate the capacitor such that it is thermally insulated from the bulk silicon. For this, part of the back surface may be etched with KOH or reactive ion etching (RIE). The choice for metal resistors was made in view of a possible economical process sequence and ease of packaging: placed on the surface of the sensor, the resistors and bondpads can be fabricated in a single metallisation step together with the top electrode of the capacitor. Because the latter contains small meshes, the porous silicon dielectric can be formed as the final step in the fabrication sequence. With this combination, optimal process control of the humidity-sensitive properties of the sensor is expected.

3.3 *Electrode and resistor design*

Apart from the choice of materials, a key issue in the design of a capacitive humidity sensor is the design of the metallisation. In Fig. 4, three combinatory electrode and resistor designs are shown: (1) interdigital electrodes (IDE) with a separate resistor, (2) IDE electrodes consisting of two resistors[16] and (3) a meshed electrode with the resistor patterned around it. The value of a porous silicon parallel plate capacitor with one meshed electrode can be written as:

$$C_s = \frac{\varepsilon_0 \varepsilon_{PS}(A - A_m)}{t_{PS}}, \quad [F] \tag{8}$$

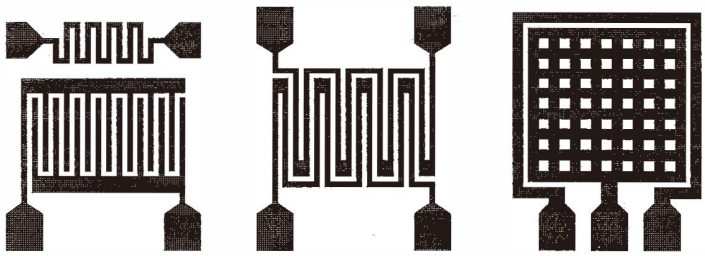

Fig. 4. Combinatory electrode and resistor layouts. Left: IDE with separate resistor. Middle: IDE consisting of two resistors. Right: meshed electrode surrounded by resistor.

where ε_0 [F/m] is the permittivity of vacuum, ε_{PS} [–] the relative permittivity of porous silicon, A [m^2] the electrode area, A_m [m^2] the total area of the meshes and t_{PS} [m] the thickness of the porous silicon. For simplicity, it is assumed that the porous silicon uniformly extends under the electrode. Hence, assuming a 1-μm-thick sheet, $\varepsilon_{PS} = 2$ and $A - A_m = 1.5$ mm^2, the capacitance is around 30 pF. If the undercut was to be taken into account, a larger value would be found because in that case t_{PS} would be effectively smaller. The choice for the metallisation was made based on two demands: (1) the metal-porous silicon contacts must be stable at elevated temperatures ($T > 100$°C) for the refreshing of the sensor, and (2) these contacts must withstand concentrated HF for about 1 min during porous silicon formation. For values of the resistors around 1 kΩ (thermoresistor) and 200 Ω (refresh resistor), a combination of chromium and gold with a temperature coefficient of $2.2 \cdot 10^{-3}$ [1/K] was found to be appropriate.[15]

4. Modelling

4.1 *Diffusion in a porous sheet*

When the sensor is placed in an environment with a certain humidity level, vapour molecules will diffuse into the pores until an equilibrium moisture content EMC [g] inside the porous dielectric is reached. The transient increase of the moisture content M [g] of the porous silicon can be estimated as a function of time with[17]

$$\frac{M(t)}{EMC} = 1 - \frac{8}{\pi^2} \sum_{n=0}^{\infty} \frac{1}{(2n+1)^2} \cdot e^{-D_m (2n+1)^2 \pi^2 t / t_m^2}, \tag{9}$$

where t_m [m] denotes the effective diffusion length into the porous sheet and D_m [m^2/s] the effective diffusivity. The EMC is defined as:

$$EMC = \xi \rho_w t_m A, \quad [\mathrm{g}] \tag{10}$$

where ρ_w [g/m^3] is the density of water. The time to reach 63% of the EMC, i.e., the first order response time, can be determined as:

$$\tau_{63} = 0.079 \cdot \frac{t_m^2}{D_m}. \quad [\mathrm{s}] \tag{11}$$

According to this approximation, the response time is proportional to the square of the EMC. In practice, however, eq. (11) may be inaccurate, because smaller pores at the surface lead to a very rapid moisture uptake but they also prevent the vapour from reaching the inside of the dielectric. This means that D_m will be much smaller than predicted by conventional chemical adsorption isotherms or the Knudsen theory.[18,19] Moreover, D_m will be a function of the film's thickness co-ordinate. This has been

confirmed by earlier researchers, who have found that the response time of 1-μm-thick microporous silicon can be on the order of one or more minutes.[20] One solution would be to tune the porous silicon morphology, so that it contains larger pores for fast diffusion and smaller pores for a large moisture uptake. This has been proposed by Richter.[21] However, a large void fraction consisting of many larger pores leads to a more nonlinear adsorption. It will therefore be useful to discuss the *EMC* as function of the *RH* and the pore radius distribution in more detail.

4.2 *Sensitivity and linearity*

The *EMC* introduced above depends on the degree of void filling, which is a function of the humidity level and the morphology of the porous dielectric. Condensation of water vapour inside a porous dielectric takes place in all pores with a radius smaller than the Kelvin radius r_K. For cylindrical pores which are closed at one end, the Kelvin radius is:[22]

$$r_K = -\frac{2\gamma M_w \cos\theta}{\rho_w RT \ln\left(\frac{p_w}{p_s}\right)}, \quad [\mathrm{m}] \tag{12}$$

where γ is the surface tension [N/m^2] and θ the contact angle. Assuming a porous dielectric with a pore radius distribution $p(r)$ between 0 and r_{max}, the volume fraction of pores filled with moisture can be approximated by[15]

$$\phi_w = \xi \cdot \frac{\int_0^{r_K} r \cdot p(r)\mathrm{d}r}{\int_0^{r_{max}} r \cdot p(r)\mathrm{d}r}, \quad [-] \tag{13}$$

Porous silicon with a certain *EMC* constitutes a random mixture of (oxidised) silicon, adsorbed, i.e., condensed, vapour and air. A capacitor with a porous dielectric consequently shows an as-measured or 'effective' value directly proportional to the effective permittivity ε_m of the mixture. The value of ε_m can be estimated by averaging electric fields throughout the mixture, using simplified representations of the size, orientation and shape of the constituent phases.[23] In Fig. 5, three simplified representations of three-phase mixtures are shown. Using the volume fractions ϕ_i, with the trivial relationship $\sum_i \phi_i = 1$, ε_m in the left and middle situations can be written as:

$$\varepsilon_m = \sum_i \phi_i \cdot \varepsilon_i \tag{14}$$

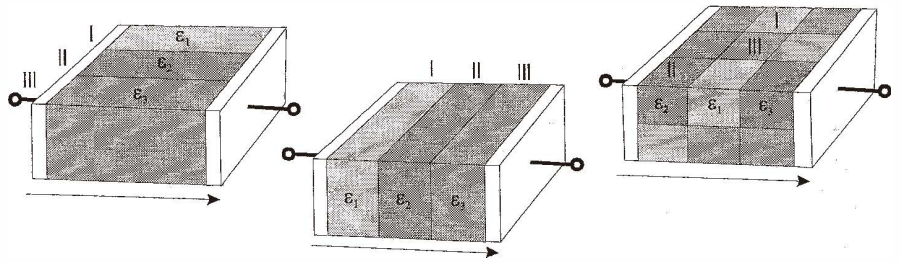

Fig. 5. Simplified representations of a heterogeneous three-phase mixture. Left: parallel circuit. Middle: series circuit. Right: fully random.

$$\frac{1}{\varepsilon_{\mathrm{m}}} = \sum_i \frac{\phi_i}{\varepsilon_i}. \quad [-] \tag{15}$$

These laws of mixtures (LOM1 and LOM2, respectively) represent the boundary values of ε_{m}. In practice, intermediate cases are found because the dispersed phase —here moisture— is randomly screened by the applied field. In other words, an accurate estimate of ε_{m} should be based on the volume fractions ϕ_i, the distribution, the shape and the orientation of the constituent phases. This is done in effective medium approximations (EMA). The most widely known EMA is due to Bruggeman. This EMA describes ε_{m} of an n-phase mixture of dispersed spherical particles as[23]

$$\sum_{i=1}^{n} \phi_i \cdot \frac{\varepsilon_i - \varepsilon_{\mathrm{m}}}{\varepsilon_i + 2\varepsilon_{\mathrm{m}}} = 0, \tag{16}$$

where ε_i is the permittivity of phase i with volume fraction ϕ_i. This EMA is a good approximation when the inclusions are on average surrounded by particles of all constituent components, i.e., in cases where $\phi_1 \ll \phi_2$ if a two-phase medium is assumed; the asymmetric Bruggeman EMA is generally appropriate for situations where $\phi_1 \approx \phi_2$. A more generalised EMA (GEMA) which accounts for the general form of the shape of the inclusions was recently proposed.[24-26] This GEMA also includes a modification accounting for possible percolation-like behaviour of the mixture. At the onset of percolation, the electrical properties of mixtures tend to change rapidly from those of the host's properties to those of the dispersed phase. This phenomenology is often observed in metal-insulator mixtures.[26] In a porous dielectric, percolation may be observed for a pore volume with numerous interconnecting pores, and hence this aspect is relevant for the choice of the dopant level of the silicon which is used in the humidity sensor.[15] The GEMA is:

$$\sum_i \phi_i \cdot \frac{\varepsilon_i^{1/t} - \varepsilon_{\mathrm{m}}^{1/t}}{\varepsilon_i^{1/t} + \dfrac{\phi_{\mathrm{p}}}{1-\phi_{\mathrm{p}}} \varepsilon_{\mathrm{m}}^{1/t}} = 0, \tag{17}$$

where ϕ_p is the percolation volume fraction and t is a nonlinearity correction factor. So for spherical inclusions with $\phi_p = 2/3$ and $t = 1$, the GEMA reduces to the Bruggeman EMA. A comparison of these approximations is made in Fig. 6, where ε_m was calculated for a two-phase mixture with $\varepsilon_{PS} = 2$ (host material) and $\varepsilon_w = 80$ (dispersed phase). Treating the as-prepared porous silicon as host material and moisture as the dispersed phase, an estimate of the sensor's humidity-sensitivity S can be given. Noting that $0 \leq \phi_w \leq \xi$, this sensitivity can be defined as the relative permittivity sweep upon maximum moisture uptake:

$$S \equiv \frac{\varepsilon_m(\xi) - \varepsilon_m(0)}{\varepsilon_m(0)}, \quad [\%] \tag{18}$$

where $\varepsilon_m(0)$ is the permittivity of the porous silicon in vacuum. Taking $\xi = 60\%$, Fig. 6 predicts that the sensitivity of porous silicon filled with 60% dispersed moisture lies around 500% (EMA), 1400% (GEMA, $\phi_p = 1/3$, $t = 1.5$) or 2400% (LOM1). The relation between these figures and the porous silicon formation parameters is discussed in more detail below.

4.3 *Temperature effects*

As mentioned above, the *EMC* is expected to increase with temperature. The reason for this is the fact that very small micropores form energetic barriers with height E_b which are more likely to be passed at elevated temperature. The amount of vapour molecules passing such a barrier can be estimated with:[27]

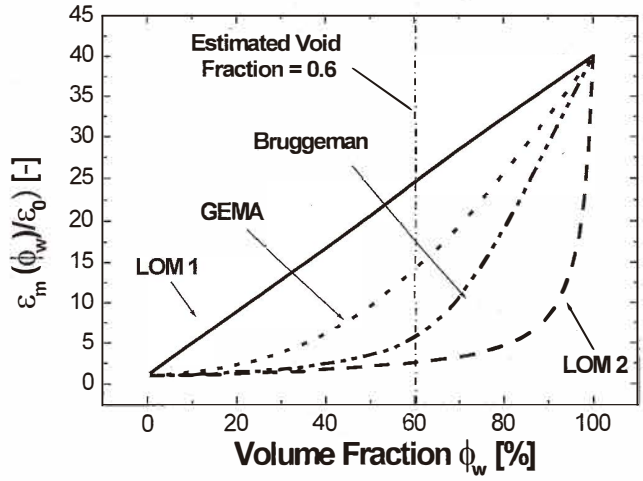

Fig. 6. Comparison of four approximations of the effective permittivity ε_m of a two-phase mixture with $\varepsilon_i = 2$ and $\varepsilon_w = 80$ as a function of the volume fraction ϕ_w.

$$\frac{\partial n}{\partial t} \propto e^{-(E_b/RT_e)}. \tag{19}$$

In equilibrium, there is a zero net flux, but if the sensor temperature T_s is higher than T_e, the *EMC* will change. Whether it will increase or decrease depends on the morphology of the porous silicon. However, in general, part of the vapour will effuse if $T_s > T_e$. The reason for this twofold. First, the Kelvin radius at higher temperatures is somewhat smaller (less condensation), and secondly there is thermal diffusion towards the environment. On the other hand, it may be that the *EMC increases* for small temperature differences because more vapour will be able to reach the interior of the dielectric, as described by eq. (19). However, at the limit, when $T_s \gg T_e$, it is expected that the effective diffusivity changes sign and all vapour is effused. The control of this process requires feedback of the temperature measurement, which can be done with the metal resistors or with the refresh resistor itself.

4.4 *Electrical equivalents*

In the first order approximation, the resistor values can be determined with:

$$R(T) = R_0\left[1 + \alpha(T - T_0)\right], \quad [\Omega] \tag{20}$$

where α is the linear temperature coefficient [1/K] and R_0 and T_0 the reference resistance and temperature, respectively. With $\alpha = 2 \cdot 10^{-3}$, a 1 kΩ resistor changes to 2 [Ω/K], which can easily be determined with electronics, for example, relaxation oscillators.[28] When electrical power is applied to the refresh resistor, entropy ('heat') flows into the bulk silicon and the package and the temperature increases. In Fig. 7, an electrical equivalent of the thermal properties of the packaged sensor is shown; estimated values of the components are summarised in Table 1. With this circuit, the transient thermal behaviour of the sensor can be found as:

$$T_s(t) = T_\infty \cdot \left(1 - e^{-\frac{t}{\tau}}\right). \quad [\mathrm{K}] \tag{21}$$

Here, T_∞ denotes the new equilibrium sensor temperature,

$$\begin{aligned} T_\infty &= P \cdot R_s^T \qquad\qquad \text{for } R_c = \infty \\ T_\infty &= P \cdot \frac{R_s^T R_p^T}{R_s^T + R_p^T} \quad \text{for } R_c = 0 \end{aligned} \quad [\mathrm{K}] \tag{22}$$

and τ the thermal response time:

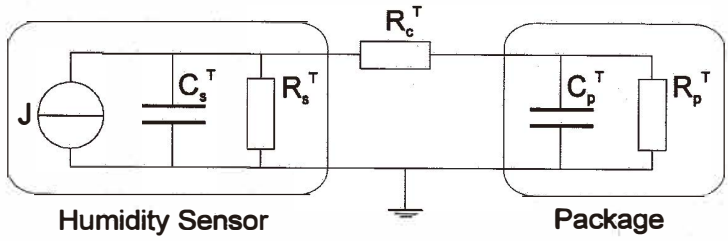

Fig. 7. Electrical equivalent of the thermal behaviour of the sensor.

Table 1
Electrical equivalents of the thermal properties of the sensor.

Component	Equivalent	Symbol	Formula	Value
		Humidity Sensor		
Refresh Power	Current Source	J	J = P	variable
Thermal Capacitance	Capacitance	C_s^T	$\rho_{Si} \cdot c_{Si} \cdot V_s$	$5.5 \cdot 10^{-3}$
Thermal Conductance	Conductance	$1/R_s^T$	$k \cdot A_s$	1/600
		Package (TO8)		
Thermal Capacitance	Capacitance	C_p^T	$\rho_p \cdot c_p \cdot V_p$	$C_p^T = 10 \cdot C_s^T$
Thermal Conductance	Conductance	$1/R_p^T$	$k \cdot A_p$	1/150
Contact Conductance	Conductance	$1/R_c^T$	$k \cdot A_c$	0 or ∞
k = convection [$W/m^2 \cdot K$]; c_{Si} = specific heat capacitance silicon [$J/kg \cdot K$]; V_s = volume sensor [m^3]; ρ_{Si} = density of silicon [kg/m^3]; subscripts 'p' for the package properties.				

$$\tau = R_s^T C_s^T \qquad \text{for } R_c = \infty$$
$$\tau = \left(C_s^T + C_p^T\right) \cdot \left(\frac{R_s^T R_p^T}{R_s^T + R_p^T}\right) \qquad \text{for } R_c = 0 \quad [\text{s}] \tag{23}$$

with C_s^T and C_p^T the thermal capacitances of the sensor and the package, and R_s^T and R_p^T the corresponding loss resistances, respectively. The value of the current equals that of the refresh power P. The resistor R_c was included to account for the nonideal thermal contact between sensor and package. The sensitivity of the resistors with respect to temperature changes induced by the refresh power can be calculated with:

$$T_\infty - T_e = R_s^T \cdot P, \quad [\mathrm{K}] \tag{24}$$

if R_c and R_p^T are infinite. Experimentally, it can be found that a sensor packaged on a standard TO8 housing increases by approximately 0.2 [K/mW] and a sensor with a radiator-like back surface packaged on perforated PCB by approximately 1.5 [K/mW].[29] Recognising that the sensor can also be used for resistive humidity measurement, a total of six operation modes of the sensor can be defined (see Table 2).

Table 2
Definition of operation modes of the humidity sensor.

Mode	Measurement	T_s	P	T_s-T_e
I	capacitive	variable	none	$T_s = T_e$
II	capacitive	constant	variable	$T_s \geq T_e$
III	capacitive	variable	constant	$T_s \geq T_e$
IV	resistive	constant	variable	$T_s \geq T_e$
V	resistive	variable	constant	$T_s \geq T_e$
VI	'refresh'	variable	'boost'	$T_s \gg T_e$

5. Fabrication and Packaging

5.1 *General description*

The fabrication sequence of the sensor is schematically presented in Fig. 8. As starting substrates, low-doped p-type (2–10 Ωcm) silicon wafers are used. First, a 1-μm-thick thermal oxide layer is deposited and patterned, whereby the capacitor area is opened. After smoothening the oxide with a 1% HF dip, 200 nm LPCVD Si_3N_4 is deposited, followed by 1 μm PECVD SiO_2 on the front surface. The Si_3N_4 is then etched in H_3PO_4 in such a way that it completely covers the thermal oxide. This step is important, because the oxide will attacked during porous silicon formation. Furthermore, the step coverage must be smooth for the metallisation. Removal of the remains of the PECVD mask is then followed by implantation and annealing of a high dose of boron (80 keV, 10^{15}) on the back surface of the wafer. If the porous silicon is formed in a single cell, an additional 1-μm-thick Al layer is sputtered on the back surface, but this layer can be omitted if a double cell is used. Also, at this point it is possible to etch part of the bulk silicon to reduce the thermal capacitance of the sensor and thus improve its thermal response time (see Fig. 9 and ref. (15)). In the standard process, the implantation is directly followed by a 6.5 mm lift-off process for complete metallisation, i.e., of the resistors, the bondpads and the meshed electrode. Finally, the porous silicon is formed by electrochemical etching in a HF-containing electrolyte; this process step is discussed in more detail below.

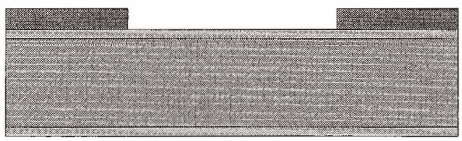

1. p-type Si, 2-10Ω cm
2. Clean, Rinse, Dry
3. Thermal Oxidation 1μm
4. 1.8μm Photoresist

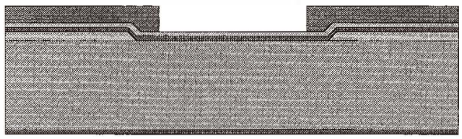

5. Wet etching oxide (BOE)
6. 1% HF dip, 3min.
7. LPCVD Si_3N_4 (200nm)
8. PECVD SiO2, front (1μm)
9. 1.8μm Photoresist

10. Wet etching PECVD SiO_2
11. Remove Photoresist (plasma)
12. Wet etching LPCVD Si_3N_4
13. Wet etching PECVD SiO_2 (rest mask)

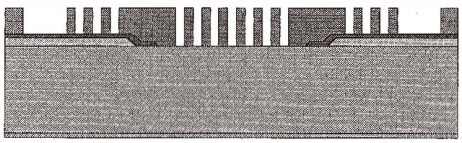

14. Boron Implantation back surface (80keV, Dose 10^{15})
15. Al sputtering, (back surface.1 μm)
16. Photoresist (6.5μm, front)

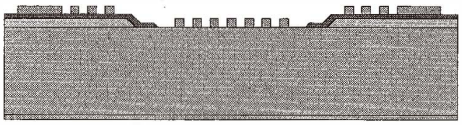

17. Sputtering Cr, Au, Cr (20, 250, 20nm)
18. Remove Photoresist (US bath, developer)

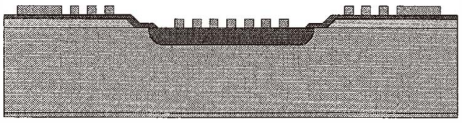

19. Porous Silicon Formation (50% HF, with surfactant, J < 30mA/cm^2)
20. Rinse, Drying, Packaging

Fig. 8. Fabrication sequence of the humidity sensor.

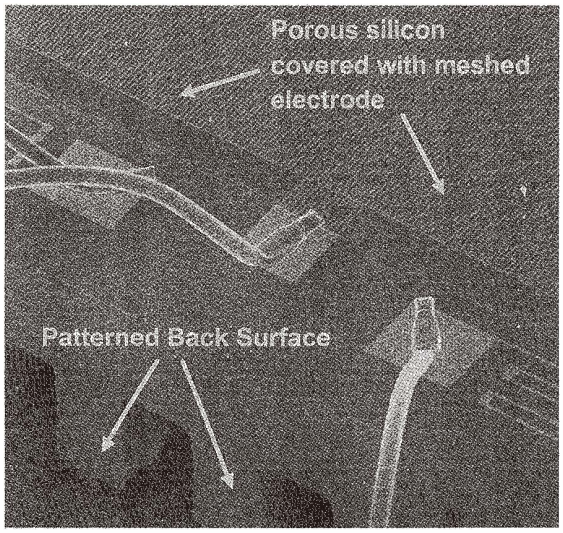

Fig. 9. SEM micrograph of the Al bond wires showing the contacts leading to the meshed electrode and the refresh resistor.

5.2 *Porous silicon formation*

One of the key reasons for using porous silicon as humidity-sensitive dielectric — apart from the substrate compatibility— is the possibility of tailoring its morphology for this purpose. As stated above, the *EMC* of a porous material is a function of the humidity, the pore radius distribution, the porosity and the temperature. In general, this implies a nonlinear relationship between ϕ_w and *RH*, as approximated by eq. (13). Furthermore, based on the field distribution throughout the porous dielectric/moisture mixture, ε_m also depends on the orientation and interconnectivity of the pores. It can thus be expected that the capacitance with a highly porous dielectric is in general a nonlinear function of the *RH*. A lower porosity will lead to more linear, but evidently also to less sensitive devices. Porous sheets with many interconnecting pores exhibit a small percolation volume fraction, and hence such sheets exhibit a higher sensitivity and improved linearity at the same porosity and pore size distribution. Confined to microporous and mesoporous silicon, one can assume the following with respect to the formation conditions of porous silicon.

5.2.1 *Microporous silicon*

In a previous work, it was shown that the porosity of electrochemically formed porous p-type silicon depends only slightly on current density and HF concentration.[4] During the anodic formation of porous silicon, holes are abundant, and the pore growth is fully random until stopped by what is assumed to be a quantum confinement effect, i.e., an effective widening of the band gap in the nm-sized remaining silicon skeleton.[3] This

self-sustaining process is an important advantage for standard process control (SPC) of the sensor, and so the sensitivity and linearity can be tailored almost completely by the current density and surfactant. A very high humidity-sensitivity of microporous silicon is hence expected because of (i) its low permittivity, (ii) its high porosity, and (iii) the occurrence of percolation-like behaviour as interpreted in terms of the regularity of the pore structure. To guarantee a rapid adsorption, the microporous silicon should be very thin (< 1 μm) and the electrodes should contain openings to allow for rapid diffusion.

5.2.2 *Mesoporous silicon*

As the pore growth in p^+-type silicon becomes more directed by electrical fields at pore tips, the influence of current density and dopant level becomes more pronounced than with p-type silicon.[4] Though this is a disadvantage for the SPC of the electrochemical etching, the mesoporous sheet that develops has clear advantages where the transient properties are concerned. However, abundant larger pores will also lead to a more nonlinear adsorption according to the Kelvin theory. Further, no percolation-like effects are expected in this type of porous Si, but because the pores, and thus the condensed vapour, are more oriented in the direction of the applied field (assuming a parallel-plate capacitor), this may not be measurable in terms of the sensitivity. It has been shown that anodising p^+-type silicon at low current density leads to a smaller mean pore radius, a smaller void fraction and hence to a smaller capacitance sweep.[2] In summary, the humidity-sensitivity of mesoporous silicon is expected to be lower than that of microporous silicon, because of (i) its higher permittivity, (ii) its lower porosity and (iii) the absence of interconnecting pores.

The properties of the p-type porous silicon sensor presented here were tailored with the anodic current density, the electrode design and with the use of several surfactants. The porous silicon was formed using a Teflon single cell with a meshed Pt electrode positioned about 1.5 cm from the 4-inch silicon wafer. A typical current density of 25 mA/cm^2 and an anodisation time between 45 s and 1.5 min were used to obtain approximately 1-μm-thick p-type porous silicon, as determined using a surface scanner after removal in 5% KOH. Relevant properties of the as-formed porous silicon are a porosity $\xi \approx 65\%$, a permittivity $\varepsilon_{PS} \approx 2$ and a specific resistivity $\rho_{PS} > 10^5\,\Omega$cm.[15]

5.3 *Meshed electrodes*

The meshed electrodes were realised with a layout comparable to that shown in Fig. 4 (right). A combination of 20 nm chromium, 250 nm gold and again 20 nm chromium as metallisation was used. The second chromium layer significantly improved the stability of the contacts, although small difficulties in wire bonding were observed.[29] The typical mesh size was 3 μm, which was also the characteristic size of the remaining structures.

5.4 *Wire bonding and packaging*

The sensors were wire bonded either on TO8 housings or on PCBs. SEM micrographs of the fully packaged sensors are shown in Fig. 9 (close up of the capacitor contact; this sensor was provided with a radiator on the back surface and bonded over a perforated PCB) and in Fig. 10 (complete view of the sensor on a TO8 housing). We found that Al

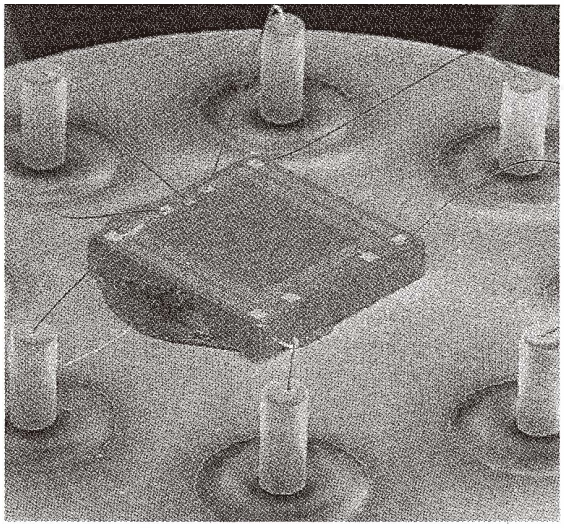

Fig. 10. SEM micrograph of the sensor packaged on a TO8 housing.

wedge-wedged wire bonds held even in humid climates and after numerous (> 25) refreshes. Minor practical difficulties were only observed while mounting sensors with a patterned back surface on perforated housings.

6. Characterization

The characterisation is confined to the humidity-sensitivity of the capacitor; properties of the integrated temperature sensors have been described elsewhere.[28,29]

6.1 *Transient properties*

Figure 11 shows some characteristic transient properties of the humidity sensor. These measurements were carried out with the sensor packaged on a standard PCB, whereby the sensor was rapidly transferred from an ambient climate (20°C, 45% *RH*) to the climate chamber (40°C, 90% *RH*). Here, a 1-μm-thick porous film formed from HF/H_2O/Fluorad FC93 was used. The as-determined response time is on the order of 1 min or less. Note that the transient maximum arises because the temperature of the climate is different from that of the ambient temperature. If they are equal, this maximum is lower, but the response time is only a little longer.

6.2 *Sensitivity, linearity and hysteresis*

The humidity-sensitivity S of the sensor was determined for several differently formed porous silicon sheets.[15] In Fig. 12, typical $C_s(RH)$ behaviour of a sheet formed from a HF/H_2O/C_2H_5OH solution is shown. The as-determined sensitivity lies around 600%,

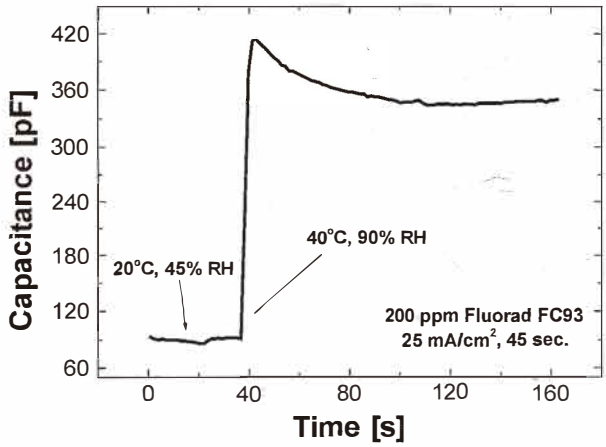

Fig. 11. Transient humidity-sensitive properties of the sensor under a step-like change from 20°C, 45% *RH* to 40°C, 95% *RH*.

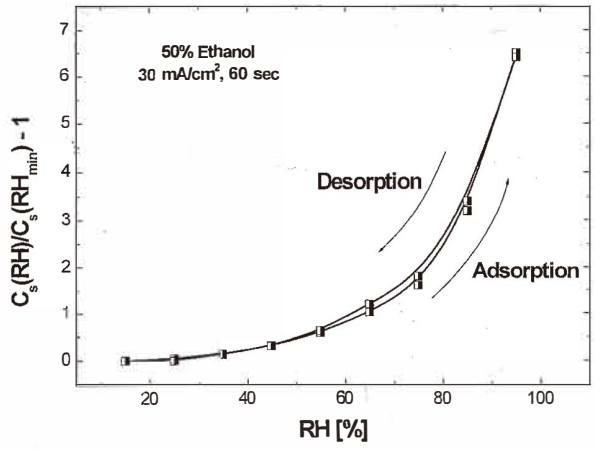

Fig. 12. Typical adsorption curve of the sensor with a 3μm meshed electrode. Porous silicon formed from HF/H_2O/ethanol.

with only a small hysteresis in the range 60–80% *RH*. In the same range, the capacitance increases much more than in the lower regimes. This behaviour indicates the presence of abundant pores in the range 3–50 nm. As the effects of percolation and capillary condensation cannot be distinguished from each other in this measurement, a conclusion with respect to the three-dimensional morphology is not made here. For this, high-resolution SEM or TEM inspection could be used to observe differences in interconnectivity.

6.3 *Refreshing the sensor*

The repeated refreshing of the sensor is represented in Fig. 13. The sensor was placed in a humid climate (90% *RH*, $T = 20°C$). After reaching equilibrium, a refresh power $P =$ 500 mW was applied for 30 s. The result of this is a rapid decrease of the capacitance, which returns to its original value after the refresh is turned off. The maximum temperature reached during this process is approximately 80°C. As this measurement shows, the adsorption properties of the porous silicon are hardly modified after several refreshes. In practice, the repeatability is improved even more by oxidation of the porous silicon during multiple (> 25) refreshes in a humid climate.

6.4 *Summary of results*

Table 3 summarises the experimentally determined properties of the sensor.

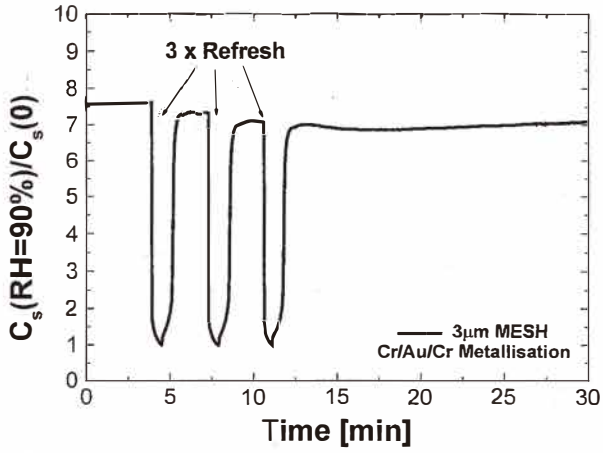

Fig. 13. Refreshing of the sensor at $RH = 90\%$ and $T = 20°C$.

Table 3
Summary of the experimentally determined sensor properties.

Surfactant*	Sensitivity	τ_{63}**	Electrode
Ethanol	510%	< 1min	Cr/Au/Cr (3µm mesh)
Triton™ X100	650%	< 1min	Cr/Au/Cr (3µm mesh)
Fluorad™ FC93	220%	< 1 min	Cr/Au/Cr (3µm mesh)

* 50% HF, 1:1 diluted (by volume) with either 98% C_2H_5OH, or a 200ppm aqueous solution of Triton X100 or Fluorad FC93.

** For approximately 1 µm thick porous silicon undergoing a step-like change from ambient (40% RH) to saturated air (95% RH).

7. Conclusions

The design, fabrication and characterisation of a humidity sensor featuring a porous silicon capacitor and integrated refresh resistor were described. The design of this sensor was based on a combination of general demands for humidity sensors, as well as on economic considerations. We presented a simple back-end process sequence, whereby the novel process, i.e., porous silicon formation, was integrated at the end of the fabrication sequence. The device can be fabricated with only two masks, whereby the complete metallisation, i.e., of the capacitor's top-electrode and the resistors, is realised in one step preceding the porous silicon formation. In this way, a simplified fabrication process was accomplished along with an optimisation of the material's properties and control.

Acknowledgements

The authors thank Eva-Maria Meyer, André Bödecker and Uwe Storm at IMSAS for their kind and valuable assistance with the realisation of the sensors.

References

1 M. I. J. Beale, J. D. Benjamin, M. J. Uren, N. G. Chew and A. G. Cullis: J. Crystal Growth **73** (1985) 622.
2 M. J. Eddowes: J. Electroanal. Soc. **280** (1990) 297.
3 L. T. Canham: Appl. Phys. Lett. **57** (1990) 1046.
4 R. L. Smith and S. D. Collins: J. Appl. Phys. **71** (1992) R1-R22.
5 A. Ulhir: J. Bell. System Tech. **35** (1956) 333.
6 W. Lang, K. Kühl and E. Obermeier: Sensors and Actuators A **21–23** (1990) 473.
7 T. Kalinowski, Z. M. Rittersma, W. Benecke and J. Binder: An advanced micromachined fermentation monitoring device: Proc. Eurosensors XIII (The Hague, The Netherlands, 13-15 September 1999) 987.
8 Th. Laurell, J. Drott, L. Rosengren and K. Lindstrom: Sensors and Actuators B **31** (1996) 161.
9 S. M. Prokes: J. Mater. Res. **11** (1996) 305.
10 C. Düscö, N. Quoc Khanh, Z. Horváth, I. Bársony, M. Utriainen, S. Letho, M. Nieminen and L. Niinistö: J. Electrochem. Soc. **143** (1996) 683.
11 J. J. Yon, K. Barla, R. Herino and G. Bomchil: J. Appl. Phys. **62** (1987) 1042.
12 R. C. Anderson, R. S. Muller and C. W. Tobias: Sensors and Actuators A **21–23** (1990) 835.
13 G. M. O'Halloran: Capacitive humidity sensor based on porous silicon, Ph.D. Dissertation, Delft University (1999).
14 P. P. L. Regtien: Silicon dew-point sensor for accurate humidity measurement systems, Ph.D. Dissertation, Delft University (1981).
15 Z. M. Rittersma: Microsensor Applications of Porous Silicon. From Humidity-Sensitive Sheet to Sacrificial Layer (Shaker Publishing, Maastricht 1999).
16 G. R. Langereis: An integrated sensor system for monitoring washing processes, Ph.D. Dissertation, University of Twente (1999).
17 J. Crank: The Mathematics of Diffusion (Clarendon Press, Oxford, 1956, 2nd ed.).
18 R. E. Cunningham and R. J. J. Williams: Diffusion in Gases and Porous Media (Plenum Press, New York, 1980).

19 M. Knudsen: Ann. d. Phys. (1908) p. 75.
20 R. C. Anderson: Formation, properties and microsensor applications of porous silicon, Ph.D. Dissertation, University of California, Berkeley (1992).
21 A. Richter: Kapazitieve Feuchtesensoren mit anorganischen Dielektrika, Ph.D. Dissertation, Technical University of Munich (1992).
22 K. Bratzler: Adsorption von Gasen und Dämpfen in Laboratorium und Technik (Theodor Steinkopf, Dresden, 1944).
23 D. A. G. Bruggeman: Teil I, Ann. der Physik **5**, Band 24 (1935), 636-679 and Teil II, Ann. der Physik **5**, Band 24 (1935) 636.
24 D. S. McLachlan: Solid State Communications **60** 10 (1986) 821.
25 D. S. McLachlan: J. Phys. C: Solid State Phys. **19** (1986) 1339.
26 D. S. McLachlan: Solid State Communications **72** 8 (1989) 831.
27 S. J. Gregg and K. S. W. Sing: Adsorption, Surface Area and Porosity (Academic Press, London, 1967).
28 Z. M. Rittersma, W. J. Zaagman, M. Zetstra and W. Benecke: A monitoring instrument with capacitive porous silicon humidity sensors, J. Smart Mater. Struct., *to be published.*
29 Z. M. Rittersma and W. Benecke: A novel capacitive porous silicon humidity sensor with integrated thermo- and refresh resistors: Proc. Eurosensors XIII (The Hague, The Netherlands, 13-15 September 1999) p. 371.